Diffusion to a Cylinder

Consider a uniform flow with velocity U and concentration c_o approaching a cylinder of radius a.. For a low Reynolds number condition (with Re << 1), the stream function near the cylinder is given by

$$\psi = AUa\sin\theta\left[\frac{r}{a}\left(2\ln\frac{r}{a}-1\right)+\frac{a}{r}\right], \tag{1}$$

where

$$A=\frac{1}{2(2-\ln R_e)}. \tag{2}$$

The diffusion equation is given by

$$\frac{v_\theta}{r}\frac{\partial c}{\partial \theta}+v_r\frac{\partial c}{\partial r}=D\left(\frac{\partial^2 c}{\partial r^2}+\frac{1}{r}\frac{\partial c}{\partial r}\right). \tag{3}$$

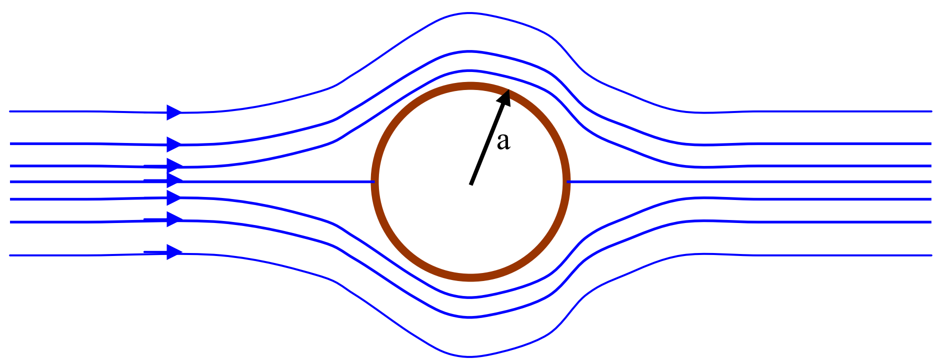

Figure 1. Schematics of a flow around a circular cylinder.

The boundary conditions for an absorbing surface are given as

$$\begin{aligned} r &= a+\frac{d}{2}, \qquad c=0 \\ r &= \infty, \qquad c=c_\infty \end{aligned} \tag{4}$$

where d is the particle diameter.

Using x, y coordinate as shown in Figure 2, we find

$$u\frac{\partial c}{\partial x} + v\frac{\partial c}{\partial y} = D\frac{\partial^2 c}{\partial y^2}, \tag{5}$$

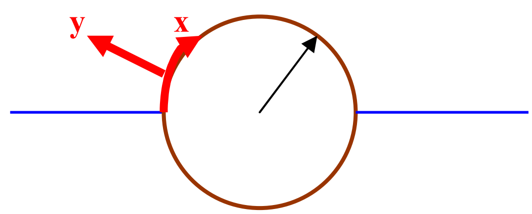

Figure 2. Surface coordinate system.

The boundary conditions given by (4) for small aerosols reduce to

$$\begin{aligned} y &= 0, \quad c = 0 \\ y &= \infty, \quad c = c_\infty \end{aligned} \tag{6}$$

Introducing the stream function ψ

$$u = \frac{\partial \psi}{\partial y}, \quad v = -\frac{\partial \psi}{\partial x}, \tag{7}$$

and using x and ψ as independent variables, one finds

$$\frac{\partial c}{\partial x} = D\frac{\partial}{\partial \psi}[u\frac{\partial c}{\partial \psi}]. \tag{8}$$

When the concentration boundary layer is thin, the stream function given by (1) may be approximated as

$$\psi \approx 2AaUy_1^2 \sin x_1, \tag{9}$$

where

$$y_1 = \frac{y}{a}, \quad x_1 = \frac{x}{a}. \tag{10}$$

Here

$$u = \frac{\partial \psi}{\partial y} = \sqrt{(\frac{8AU}{a})} \sin^{1/2} x_1 \psi^{1/2} \tag{11}$$

Equation (8) may be restated as

$$\frac{\partial c}{\partial \chi} = \frac{D}{aAU} \frac{\partial}{\partial \psi_1} (\psi_1^{1/2} \frac{\partial c}{\partial \psi_1}), \tag{12}$$

where

$$\chi = \int \sin^{1/2} x_1 dx_1, \quad \psi_1 = \frac{\psi}{2AaU}. \tag{13}$$

The boundary conditions are now given by

$$\begin{aligned} \psi_1 &= 0, \quad c = 0 \\ \psi_1 &= \infty, \quad c = c_\infty \end{aligned} \tag{14}$$

Introducing the similarity variable

$$\xi = \frac{\psi_1}{\chi^{2/3}}, \tag{15}$$

Equation (12) may be restated as

$$-\frac{AP_e}{3} \xi \frac{dc}{d\xi} = \frac{d}{d\xi} (\xi^{1/2} \frac{dc}{d\xi}). \tag{16}$$

The solution to Equation (16) is given by

$$c = \frac{c_\infty (AP_e)^{1/3}}{1.45} \int_0^{\sqrt{\xi}} \exp\{-\frac{2}{9} AP_e z^3\} dz, \tag{17}$$

where

$$P_e = \frac{2Ua}{D} = R_e \cdot S_c \tag{18}$$

is the Peclet number.

The averaged Sherwood number is given by

$$\overline{sh} = \frac{\bar{h}(2a)}{D} = 1.17(AP_e)^{1/3}, \tag{19}$$

where $\bar{h}$ is the averaged mass transfer coefficient. The collection efficiency is defined as the fraction of the particles collected from the fluid in the volume swept by the cylinder. That is

$$\eta_R = \frac{\bar{h}\pi(2a)c_\infty}{(2a)Uc_\infty} = 3.68A^{1/3}P_e^{-2/3}. \tag{20}$$

Since $P_e = 2aU/D$, it follows that $\eta_R \sim d^{-2/3}$ (or $d^{-4/3}$ for free molecular regime). Variations of $\overline{sh}/A^{1/3}$ and $\eta_R/A^{1/3}$ with P_e are shown in Figure 3.

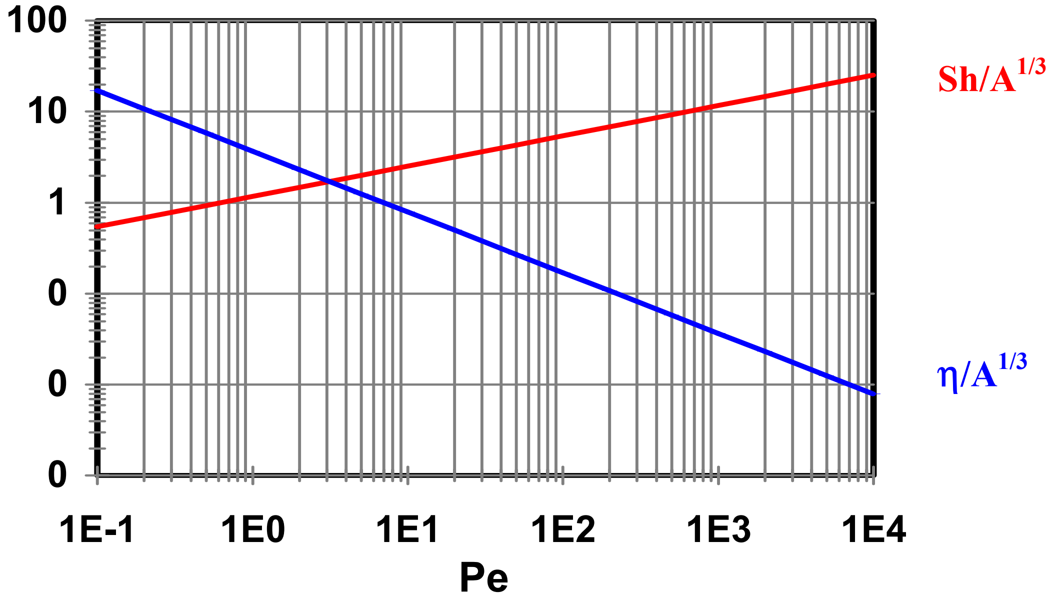

Figure 3. Variations of $\overline{sh}/A^{1/3}$ and $\eta_R/A^{1/3}$ with P_e.

Direct Interception Limit

For $P_e \to \infty$ (absence of diffusion), particles follow the fluid and deposit when a streamline passes within one radius of the surface. This is referred to as the direct interception. Schematics of interception process are shown in Figure 4.

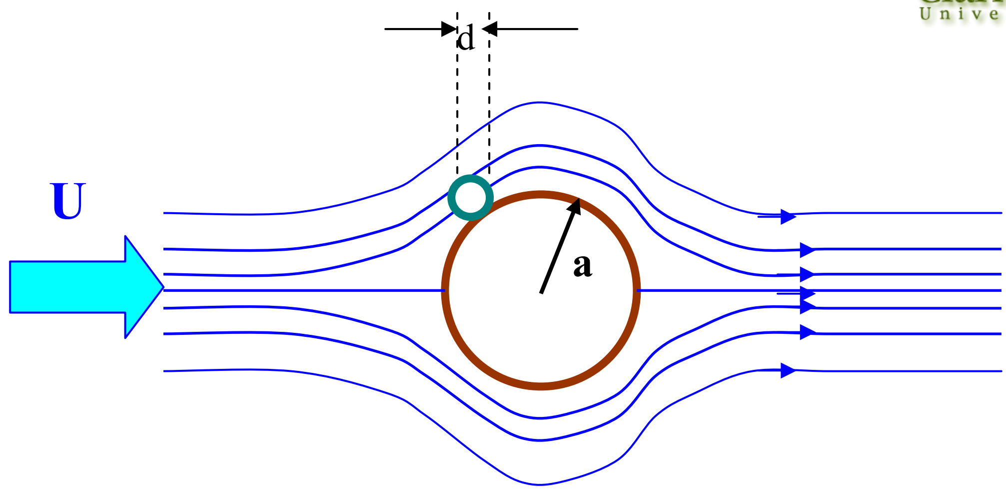

Figure 4. Schematics of interception process.

The capture efficiency then is given by

$$\eta_R = -\frac{\int_0^{\pi/2} v\,|_{y=d/2}\, dx}{Ua} = 2AR^2, \tag{21}$$

where

$$R = \frac{d}{2a}, \tag{22}$$

is the interception parameter.

Equations (20) and (21) are for the limiting conditions that the diffusion or the direct interception are dominant. They show that for fixed U and fiber diameter, the efficiency decreases with particle diameter d at first and then increases with further increase in d.

Fiber Efficiency/Filter Efficiency

The efficiency of a fibrous filter is directly related to the single fiber efficiency. For a regular array shown in Figure 5, the decrease of concentration in a length dz is given by

$$dc = -\underbrace{[\eta_R (2a) c]}_{\text{Collection by one fiber}} \underbrace{\left(\frac{\upsilon dz}{\pi a^2}\right)}_{\text{No. of fibers}}, \tag{23}$$

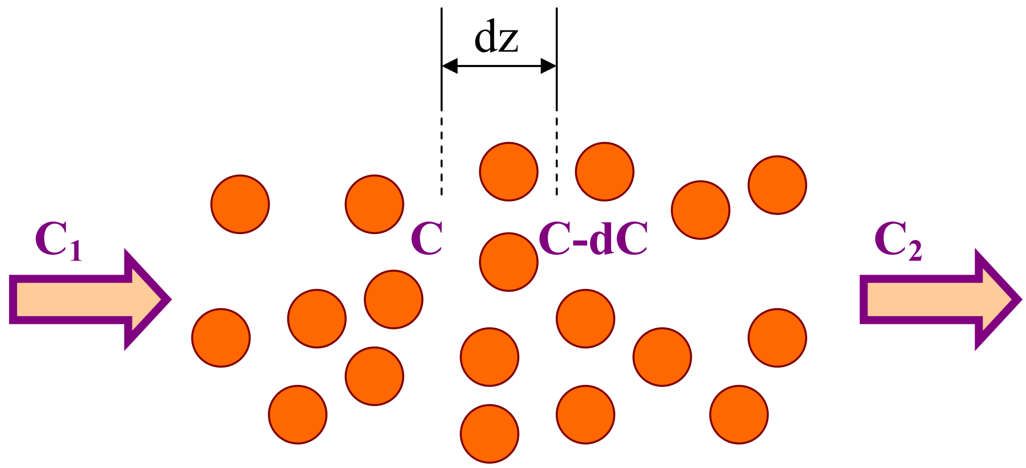

Figure 5. Schematics of gas flow through a fiber filter.

where υ is the fraction of solid (fibers). Rearranging and integrating (23), it follows that

$$\eta_R = \frac{\pi a}{2\upsilon L} \ln \frac{c_1}{c_2}, \tag{24}$$

where L is the length of the filter. For η_R the following semi-empirical equation was suggested (Hinds, 1982):

$$\eta_r(RP_e) = 1.3RP_e^{1/3} + 0.7(RP_e^{1/3})^3, \tag{25}$$

which correlates well with the data as shown in Figure 6. Note also that Equation (25) reduces to (21) as $P_e \to \infty$ and resembles (20) for $P_e \to 0$. For Re=0.1, the predictions of Equations (20) and (21) are shown in Figure 6 for comparison. It is seen that the prediction of Equation (20) for the diffusion limit is in good agreement with the result of (25) for small Peclet numbers. Similarly the prediction of Equation (21) for the interception limit asymptotes the empirical Equation (25) at large Peclet numbers.

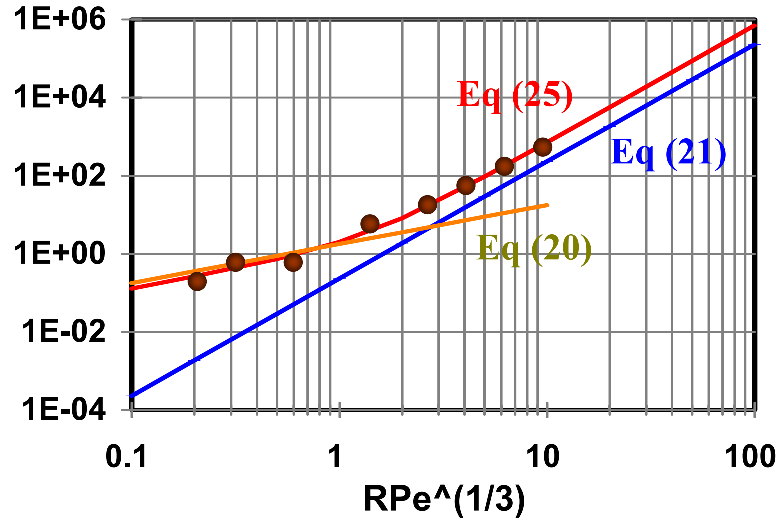

Figure 6. Variation of filter collection efficiency $\eta_r RP_e$ with $RP_e^{1/3}$.